Briefing Space Weather - 2022/02/14

Sun

Responsible: José Cecatto

02/07 – Fast (=< 550 km/s) wind stream; 4 CME can have component toward the Earth;
02/08 – Fast (=< 450 km/s) wind stream; 2 CME can have component toward the Earth;
02/09 – Fast (=< 450 km/s) wind stream; No CME toward the Earth; CME arrival on Feb, 09 at ~21:00 UT;
02/10 – Fast (=< 450 km/s) wind stream; 4 CME can have component toward the Earth;
02/11 – Fast (=< 500 km/s) wind stream; 1 CME can have component toward the Earth;
02/12 – Fast (=< 600 km/s) wind stream; 6 CME can have component toward the Earth;
02/13 – Fast (=< 550 km/s) wind stream; 4 CME can have component toward the Earth;
02/14 – Fast (=< 500 km/s) wind stream; 2 CME can have component toward the Earth;
Prev.: Fast wind expected up to February 15; for while low (25% M, 1% X) probability of M / X flares next 2 days; also, occasionally some other CMEs can present a component toward the Earth.

Responsible: Douglas Silva

CME:
● Partial halo coronal mass ejection was observed around 00:36 UT on February 11 in LASCO
imagery.
WSA-ENLIL (CME 2022-02-11T00:36Z)
● No or little impact to Earth.
Coronal holes (SPOCA):
● Coronal hole 35025 was identified by SPOCA between the 07th and 10th of

February.

● Coronal hole 34857 was identified by SPOCA between the 09th and 10th of February.

Interplanetary Medium

Responsible: Paulo Ricardo Jauer

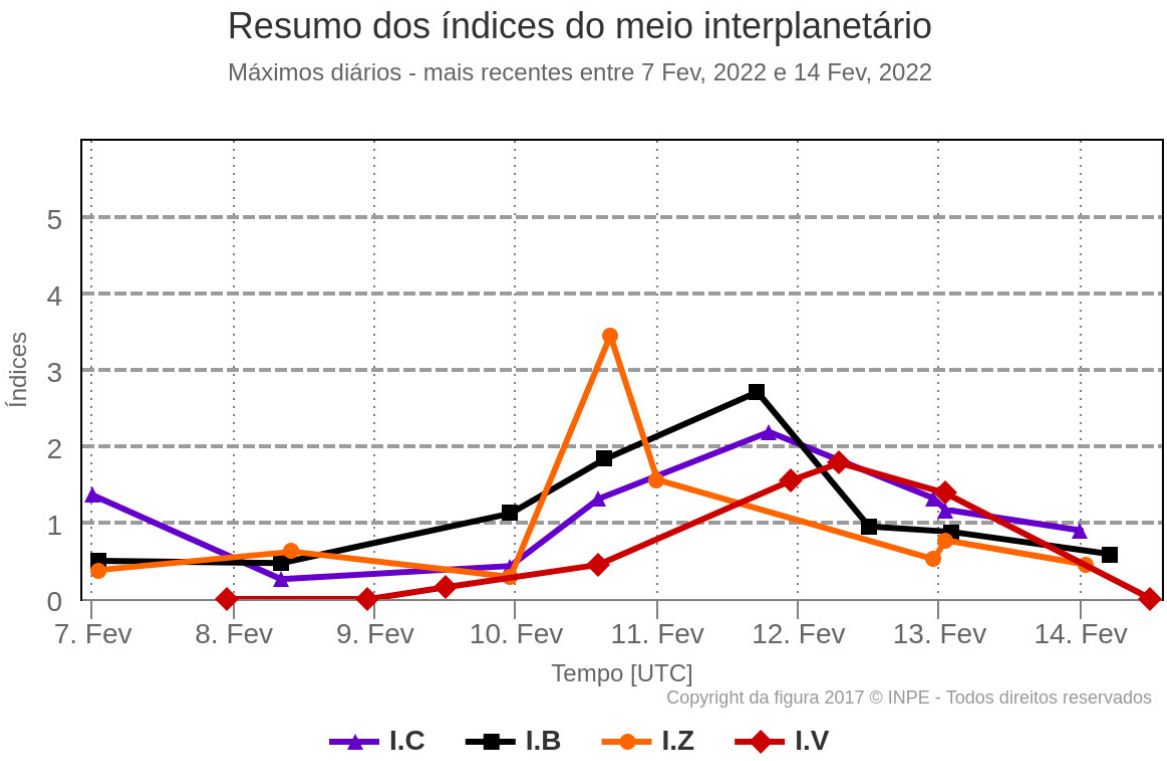

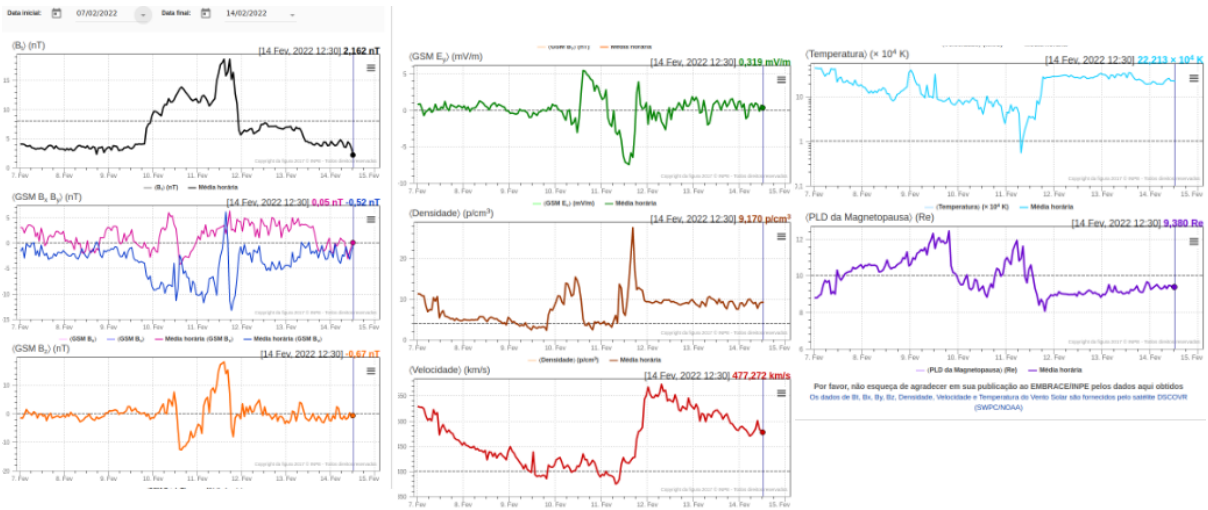

- The interplanetary region in the last week showed a moderate/high level of plasma perturbations due to the passage of the CME and HSS structures identified by the DISCOVERY satellite in the interplanetary region.
- The modulus of the interplanetary magnetic field component showed a sudden variation on February 09 at 19:30, reaching a maximum peak on February 11 at 17:30 18.54 nT, and returning to values below 10 nT on the 12th. /Feb at 00:30 6 nT.
- BxBy components do not show a clear sector switch. The by component was more active with a variation of -13.27 nT on Feb/11 at 18:30.
- The component of the bz south field showed changes in its orientation. On the 10/Feb at 14:30 the component presented the lowest value -12.53 nT, after on the 11/Feb there was a positive incursion of the component at 13:30 UT of +17.6nT. Returning on Feb/11 to negative values of -8 nT at 19:30 UT.
- The density of the solar wind showed two disturbed intervals. On Feb 10th at 10:30 UT in the amount of 15.3 p/cm³, and another on Feb 11th at 16:30 at 27.4 p/cm³.
- The solar wind speed was mostly above 400km/s during the analyzed period, with a peak around ~572km/s on 12/Feb at 07:30 UT.
- The position of the magnetopause was mostly below the typical positions. Featuring two significant compressions on February 10th and 11th at 14:30 and 19:30 UT of 8.8 and 8.0 RE respectively. Also presented on 09/Feb at 19:30 UT a 12.4 Re expansion.

Radiation Belts

Responsible: Ligia Alves Da Silva

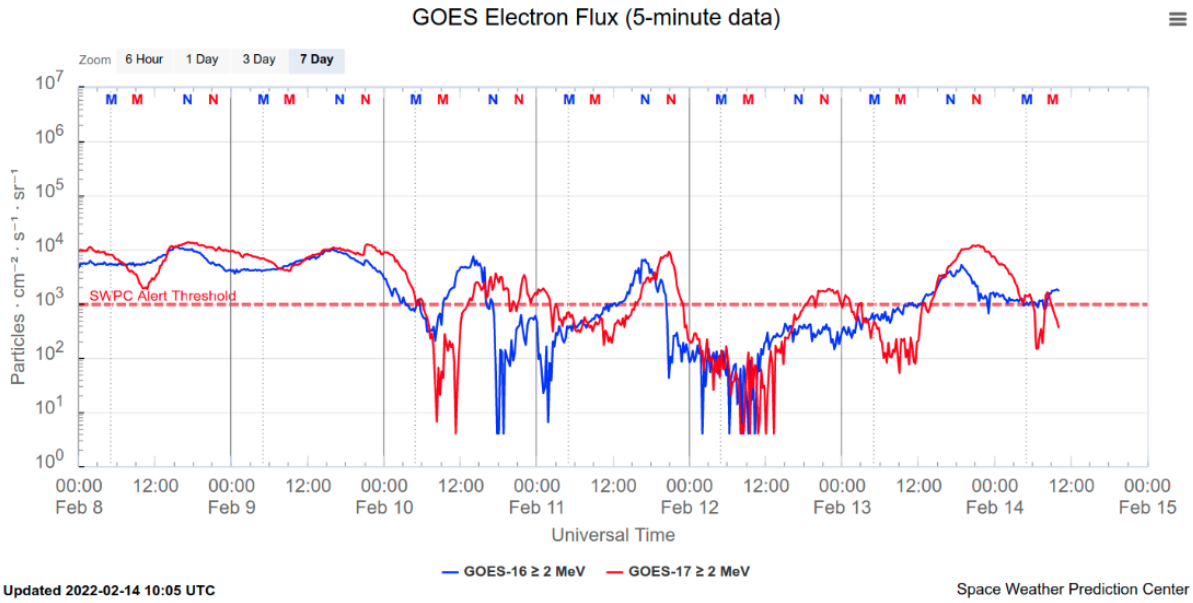

Figure 1: High-energy electron flux (> 2MeV) obtained from GOES-16 and GOES-17 satellite. Source: https://www.swpc.noaa.gov/products/goes-electron-flux

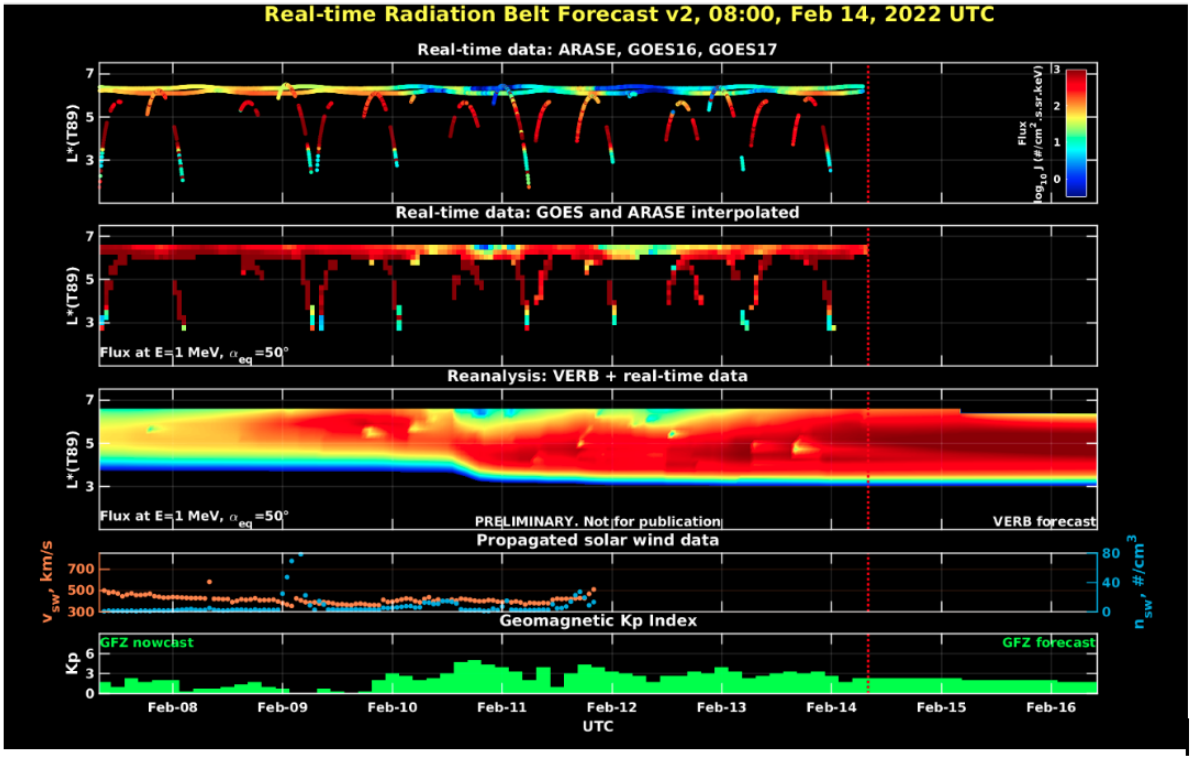

Figure 2: high-energy electron flux data (real-time and interpolated) obtained from ARASE, GOES-16, GOES-17 satellites. Reanalysis's data from VERB code and interpolated electron flux. Solar wind velocity and proton density data from ACE satellite.
Source: https://rbm.epss.ucla.edu/realtime-forecast/

High-energy electron flux (>2 MeV) in the outer boundary of the outer radiation belt obtained from geostationary satellite data GOES-16 and GOES-17 (Figure 1) is

close to 103 particles/(cm2 s sr) between February, 8th-9th. At the beginning of February 10th, a dropout of approximately three orders of magnitude is observed. After that, an electron flux increase is observed, which remained at approximately 103 particles/(cm2 s sr) until the end of February 11th. A second dropout is observed, followed by an electron flux increase that reaches 104 particles/(cm2 s sr) at 18:45 Z on February 13th.

The GOES-16, GOES-17, and Arase satellite data are analyzed and interpolated to observe the high-energy electron flux variability (1 MeV) in the outer radiation belt (Figure 2). Additionally, the VERB code rebuilds this electron considering the Ultra Low Frequency (ULF) waves' radial diffusion. The first dropout is associated with the arrival of a coronal mass ejection, while the second dropout is associated with the arrival of a high-

speed solar wind stream. These observed variabilities occurred concomitantly with ULF wave activity.

ULF waves in the Magnetosphere

Responsible: José Paulo Marchezi

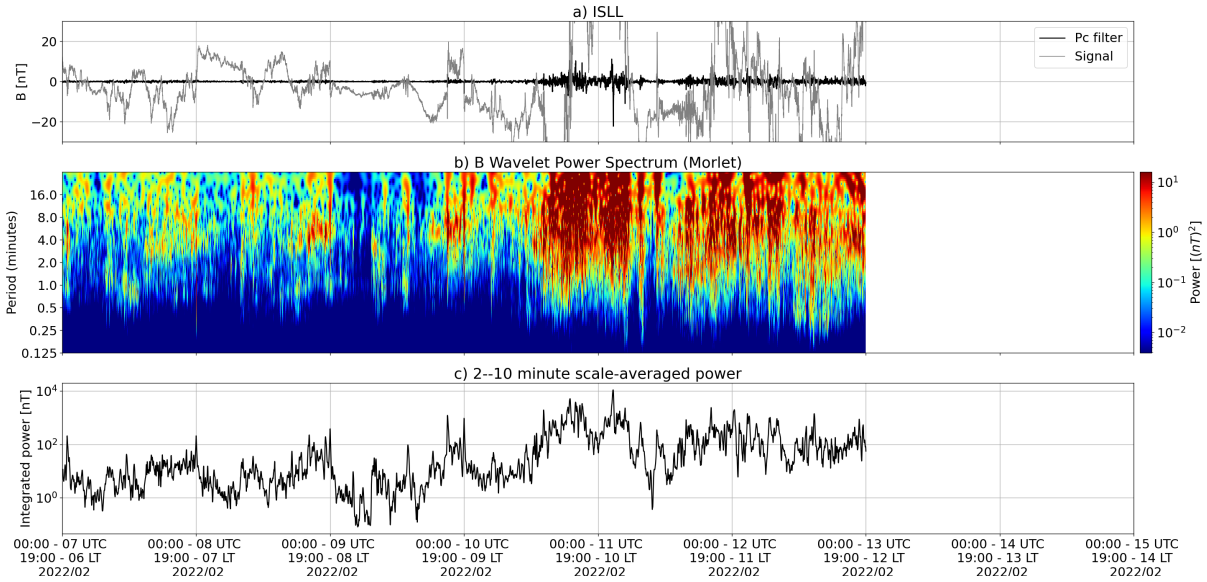

a) signal of the total magnetic field measured in the ISLL Station of the CARISMA network in gray, together with the fluctuation in the range of Pc5 in black. b) Wavelet power spectrum of the filtered signal. c) Average spectral power in the ranges from 2 to 10 minutes (ULF waves).

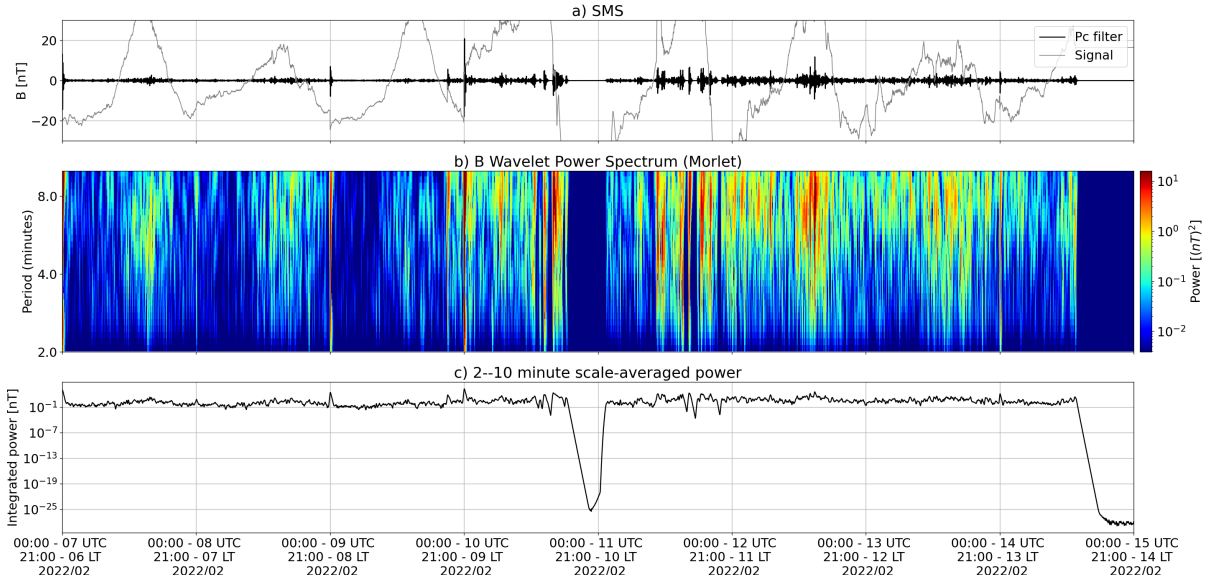

a) signal of the total magnetic field measured in the SMS Station of the EMBRACE network in gray, together with the fluctuation in the range of Pc5 in black. b) Wavelet power spectrum of the filtered signal. c) Average spectral power in the ranges from 2 to 10 minutes (ULF waves).

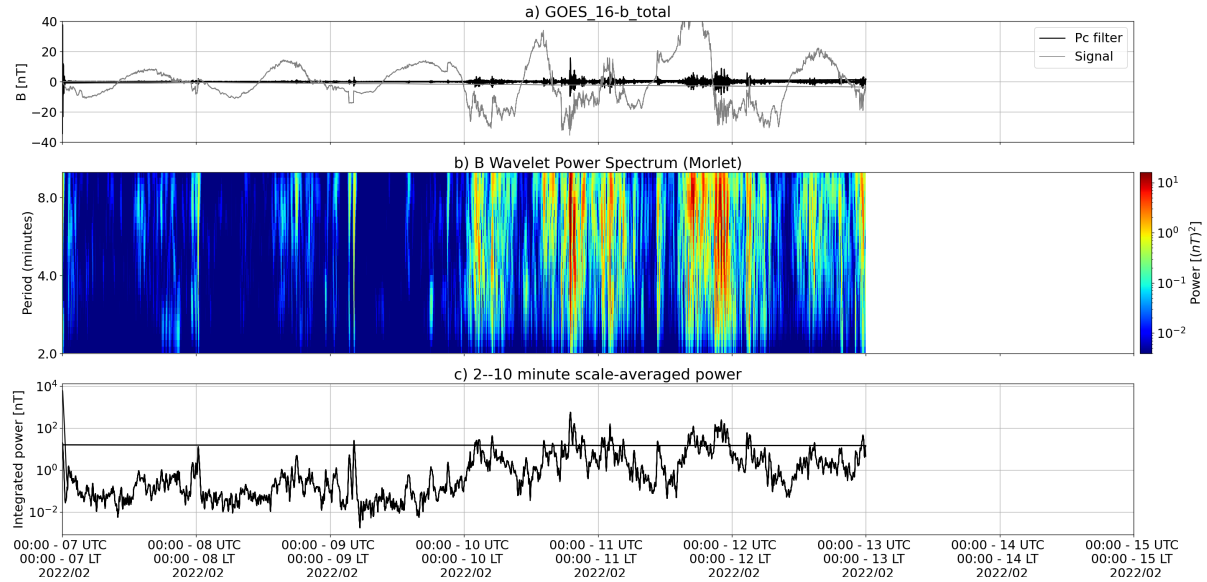

a) signal of the total magnetic field measured by the GOES 16 satellite, together with the fluctuation in the range of Pc5 in black. b) Wavelet power spectrum of the filtered signal. c) Average spectral power in the ranges from 2 to 10 minutes (ULF waves).

The ULF indas activity shows an increase in power from the 10th of February, where there are small shocks, which are mainly visible at high latitudes, as impulsive pulsations with short duration. On the 11th, there is a greater power of waves in the Pc5 band that last for a long period, which may be associated with the interaction of a CME with the Earth's amagnetosphere. These waves are the result of a disturbance in the equatorial currents, seen by the GOES satellite and in low-latitude

magnetometers in the EMBRACE network, and also a result of the intensification of the auroral currents, detected by magnetometers at high latitudes (ISLL-CARISMA).

Geomagnetism

Responsible: Livia Ribeiro Alves

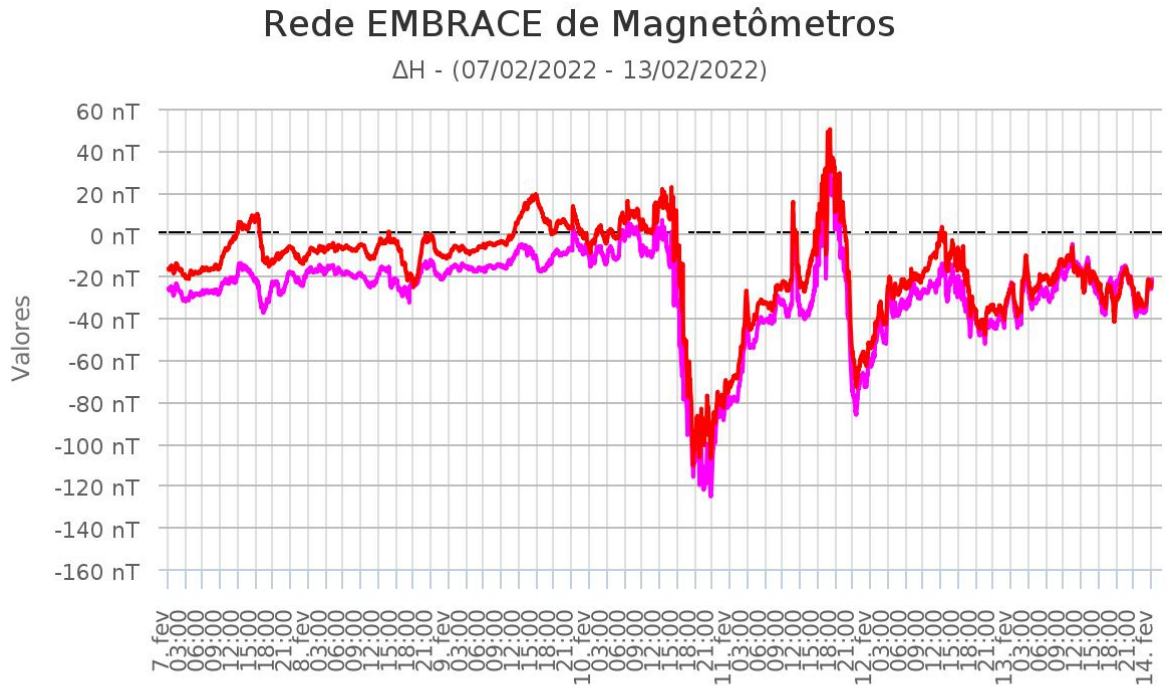

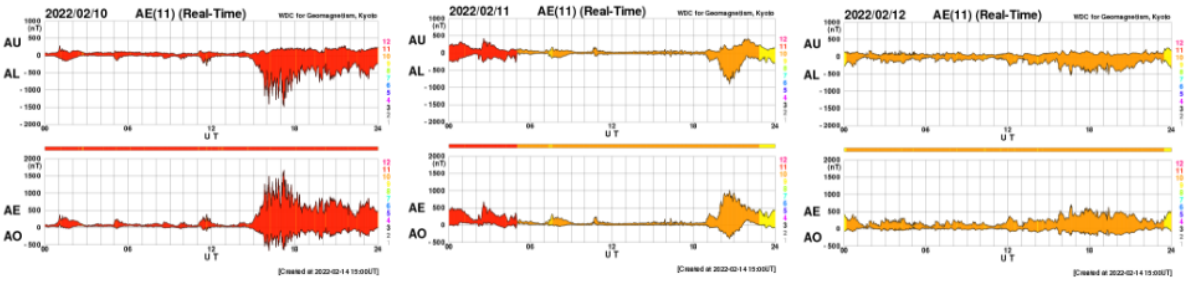

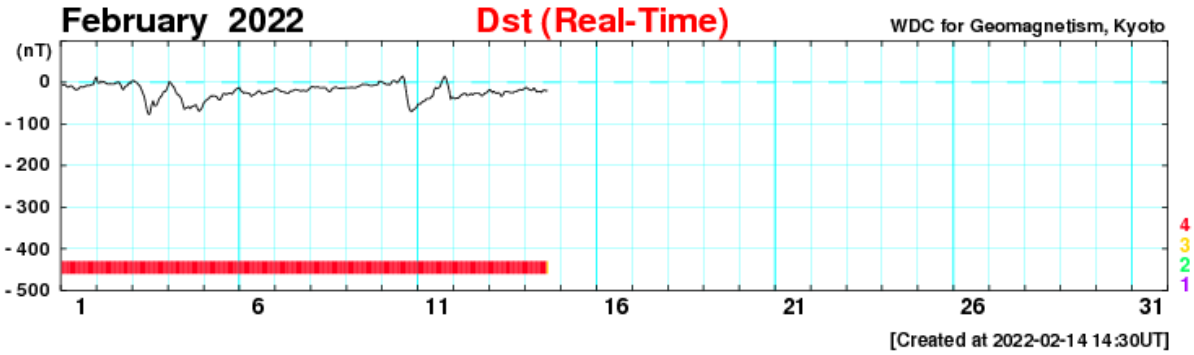

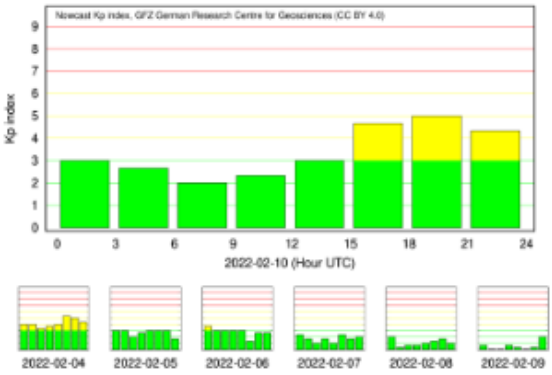

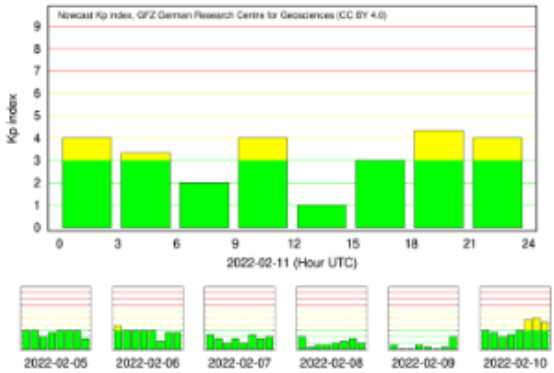

Geoelectric field 10 and 11/02

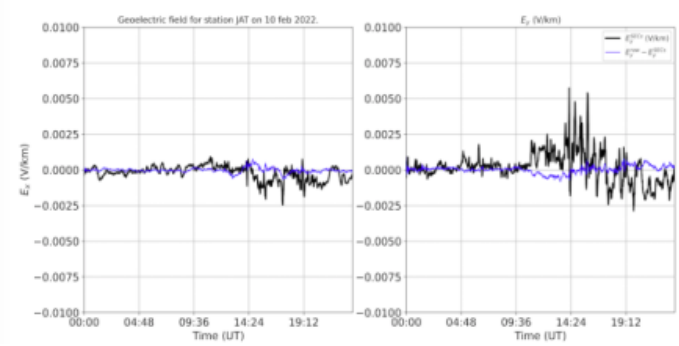

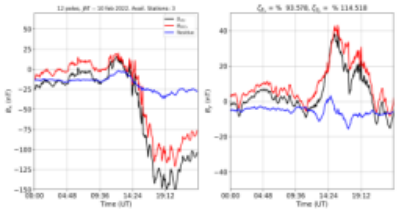

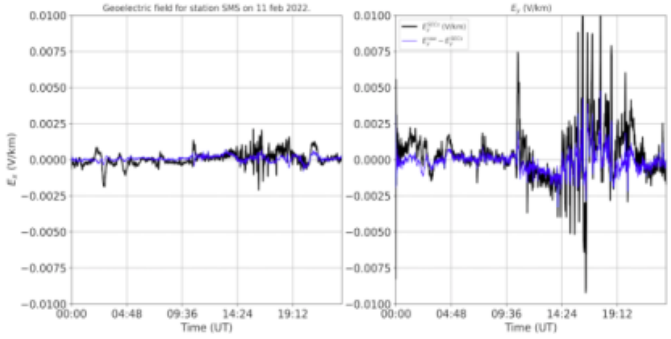

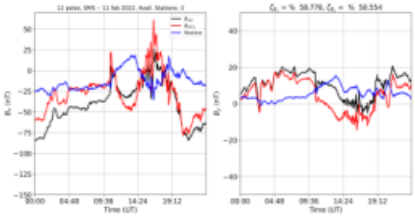

Geoelectric field 03 and 04/02

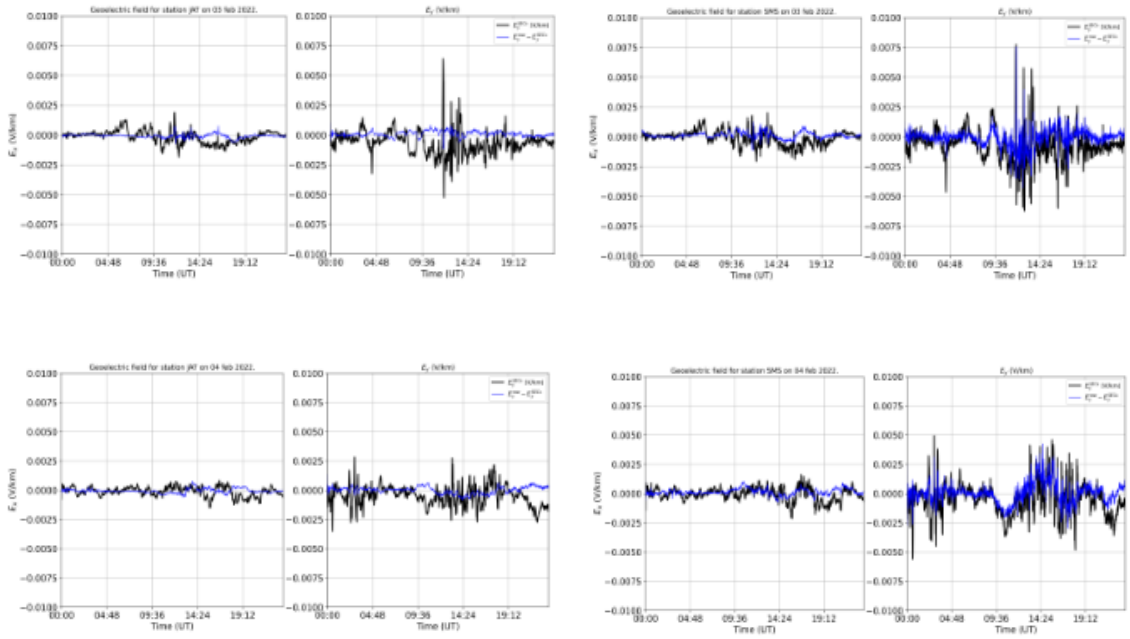

- Data from the Embrace magnetometer network showed instabilities throughout the period:
  - 10 Feb, H component, in all seasons, reached down to -120 nT
  - 11 Feb H component enhanced up to +40nT, followed by a deacrease in all stations, down to -80nT
  - days 12 and 13 geomagnetic storm recovery phase
- Geomagnetic activity reached G1 storm level on 10 and 11 Feb, with the Dst index reaching its minimum value of -70 nT on 10 Feb. The highest Kp of the week was 5o recorded on Feb 10
- Auroral activity was intensified on days 10,11.
- Magnetic field measured in the orbit of the GOES satellite showed disturbances in the period from 10 to 14 Feb.
- Induced geoelectric field was calculated for JAT and SMS stations, on days 10 and 11 respectively. The geoelectric field reached 0.010 V/km in SMS on 02/11.

Ionosphere

Responsible: Laysa Resende

Boa Vista:

- There was not occur spread F during on days 11, and 12.
- The Es layers reached scale 4 on day 07.

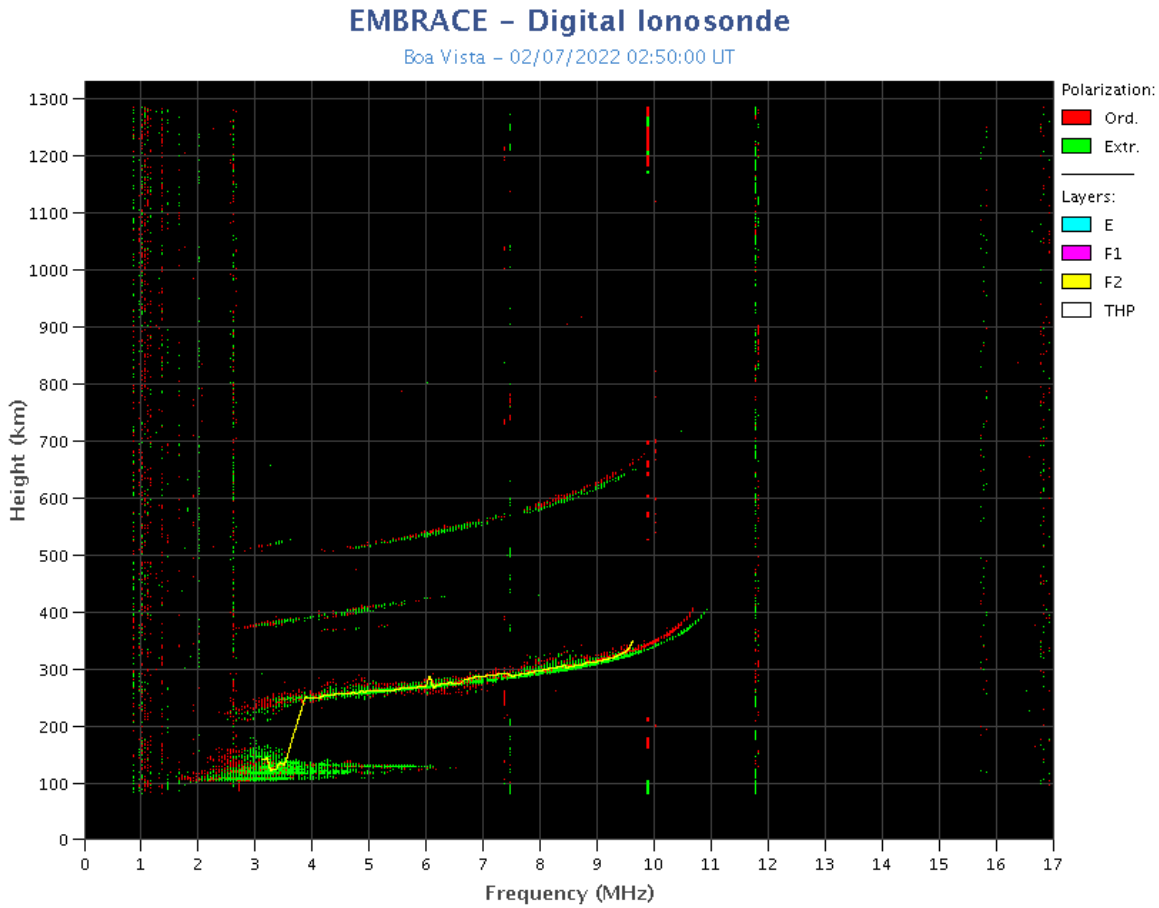

Cachoeira Paulista:

- There were spread F on days 09, and 10.
- The Es layers reached scale 3 on days 10, and 11.

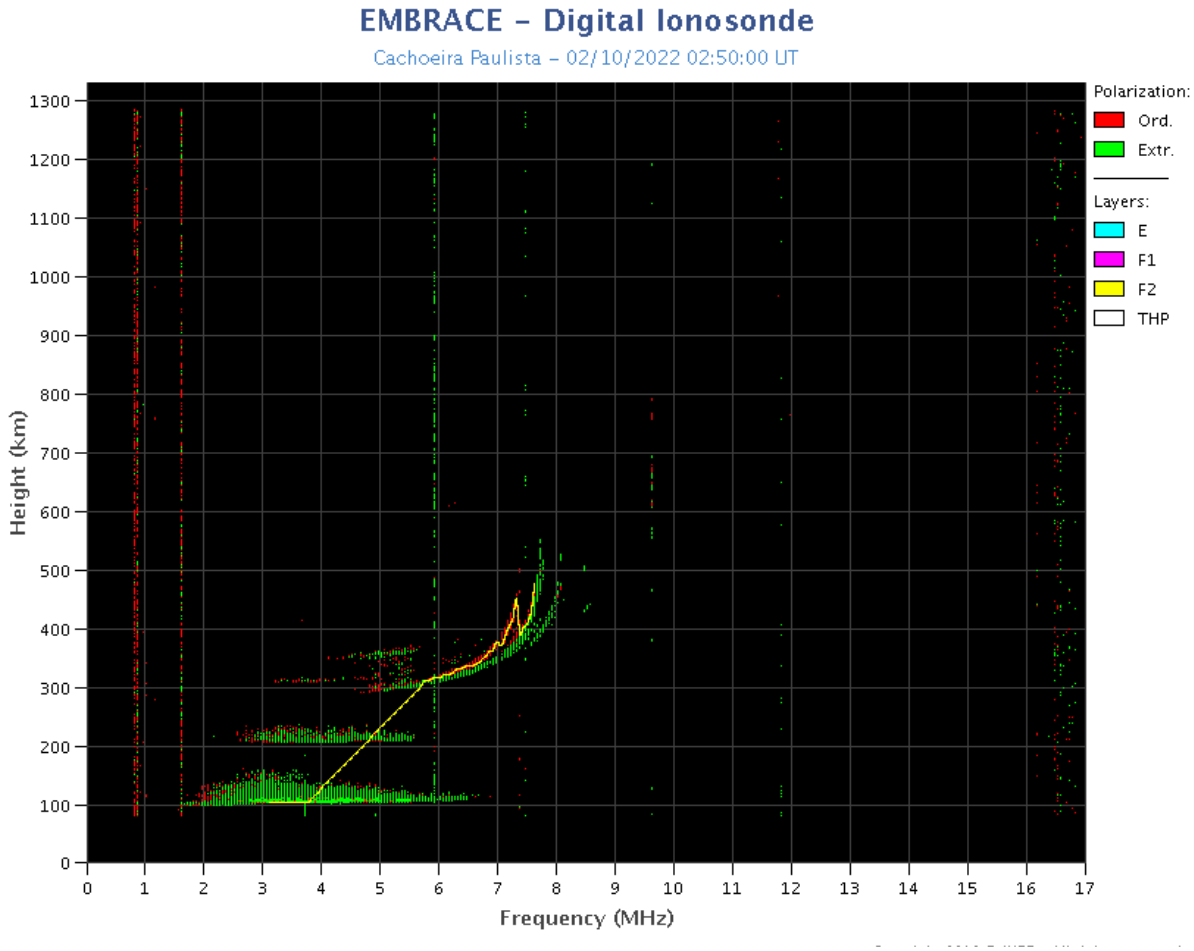

São Luís:

- There were spread F during all days in this week.
- The Es layers reached scale 3 on days 10, and 13.

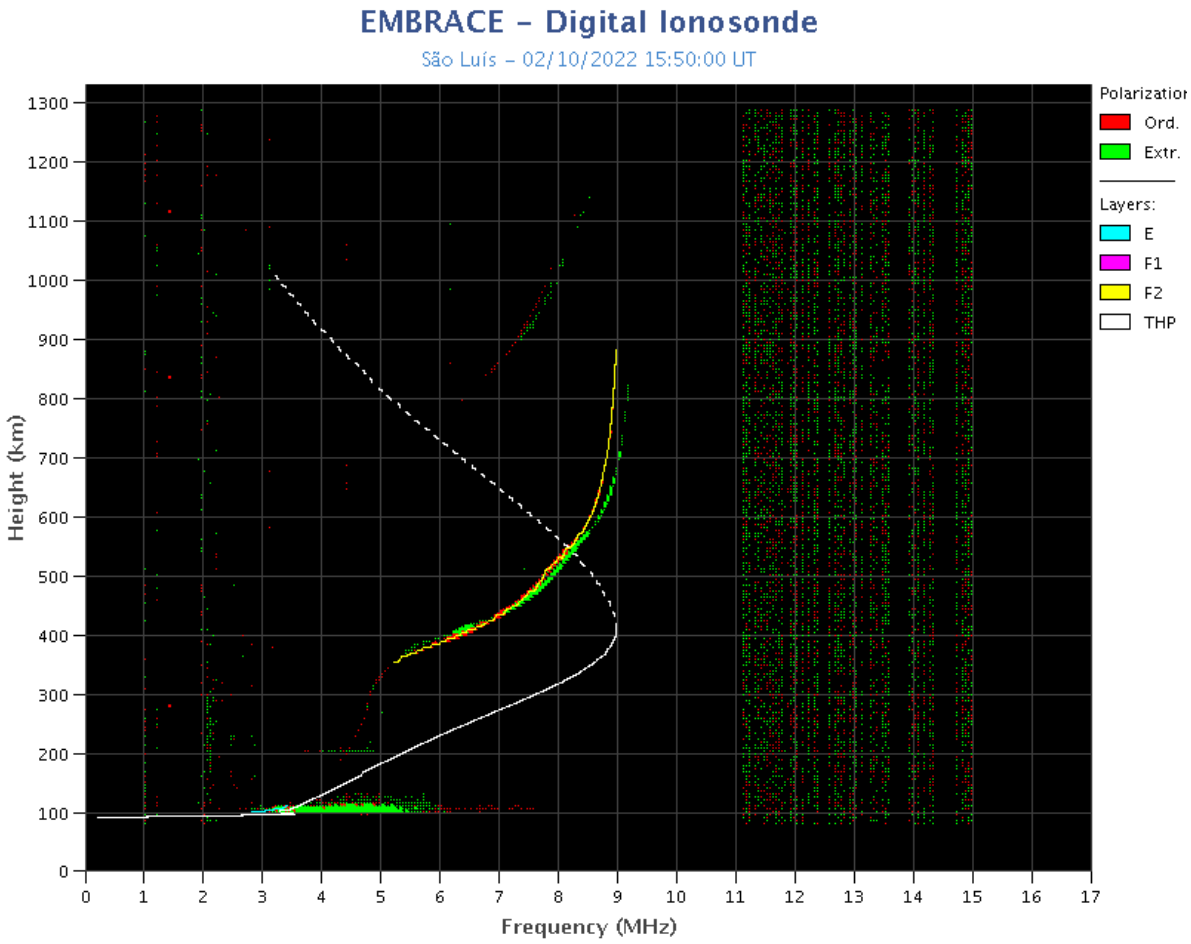

Scintillation S4

Responsible: Siomel Savio Odriozola

In this report on the S4 scintillation index, data from SLMA in São Luíz/MA, STNT in Natal/RN, UFBA, in Bahía/BA e SJCE in São José dos Campos/SP are presented. The S4 index tracks the presence of irregularities in the ionosphere having a spatial scale ~ 360 m.

At the UFBA station, data were only acquired during February 11-12. On the SLMA station, the available data appears from February 9th. Both in SLMA and STNT S4 index values show scintillation effects every day after sunset until day 10. Scintillation events are visible again on the 13th and 14th (Figure 1). In the case of the SJCE station, scintillation events, affecting few satellites of the GPS constellation, were detected in the early evening hours of the 7th, 8th, and 9th. Figure 2 shows the satellites that contributed with the highest S4 values to the SLMA, STNT and SJCE stations during 02/9-10/2022.

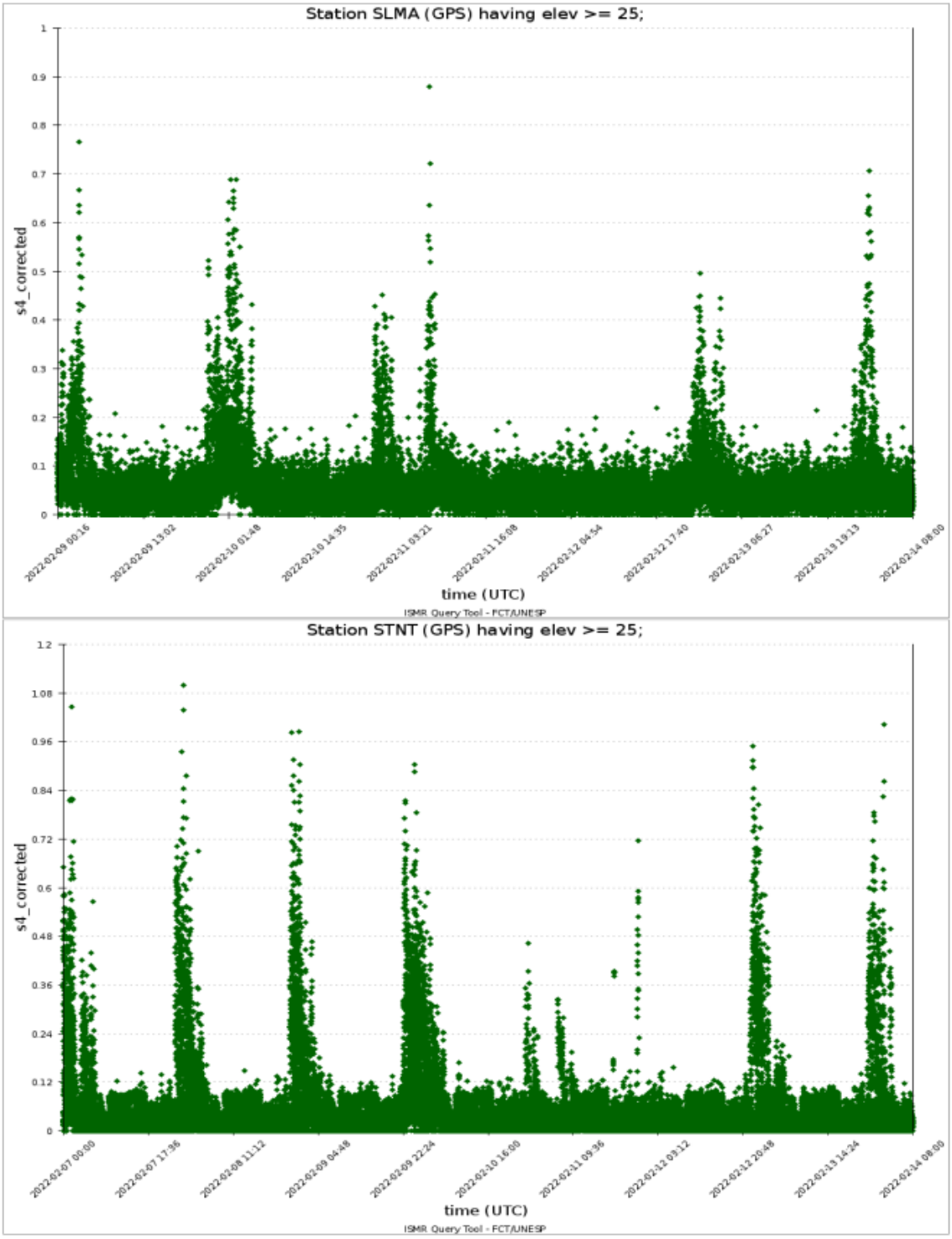

Figure 1: S4 index values for the GPS constellation for the station SLMA (upper panel) and STNT (lower panel) during the week 02/07—02/14/2022.

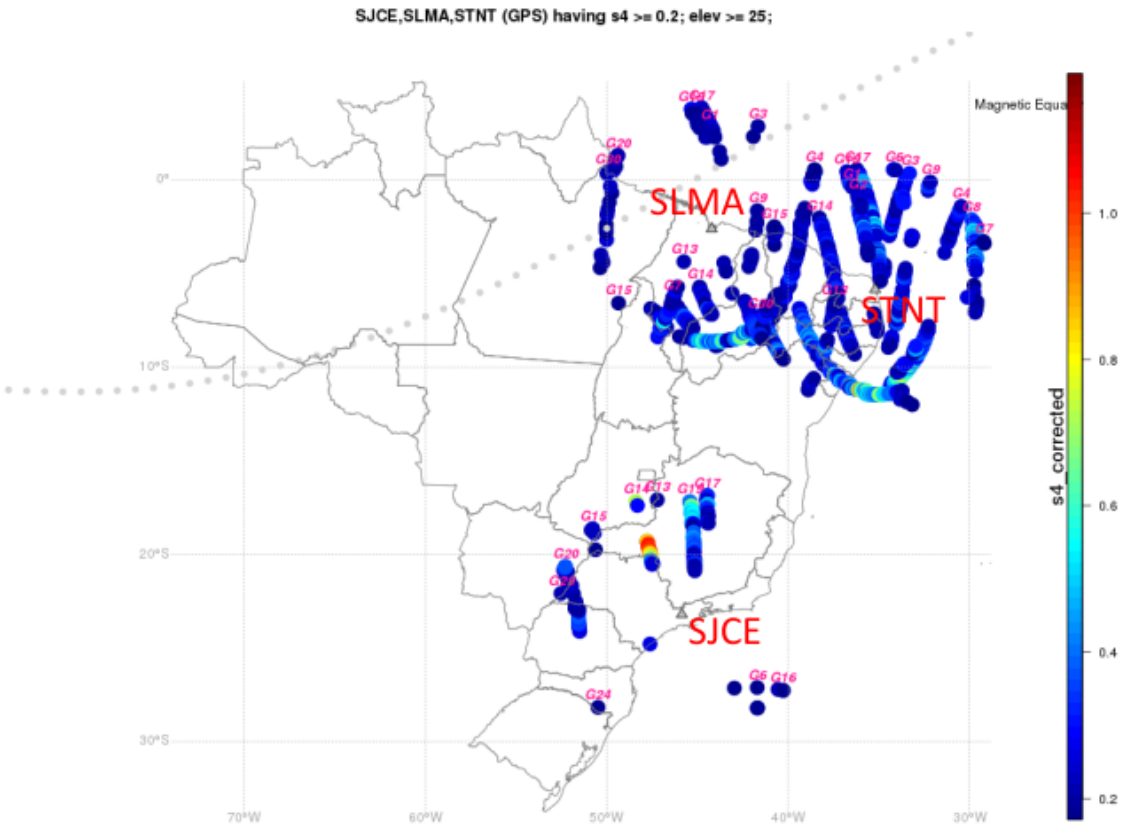

Figure 2: Map of S4 values > 0.2 for the GPS satellites with elevation > 25° in the receiver's field of view of SLMA, STNT and SJCE stations between 2200 UT on 02/9 until 0800 UT on 02/10/2022.

Imager

Responsible: Cosme Alexandre Figueiredo

The week between February 6th and 12th is the Moon period, so observations are limited to the end of the night.

Between February 6th and 10th, 2022, plasma bubbles were observed by the All-sky imagers over São João do Cariri and Bom Jesus da Lapa. While day 11 no plasma bubbles were observed and day 12 was cloudy. It is worth noting that the 9th in Bom Jesus da Lapa had no observation due to technical problems.

On the other hand, the Cachoeira Paulista observatory was cloudy throughout the analysis period. Finally, the São Martinho da Serra observatory observed plasma bubbles between days 6 and 9, however, on days between 10 and 11 no plasma bubbles were observed and day 12 was cloudy.

Between the 6th and 12th of February 2022, TEC maps show signature plasma bubbles. Day 11 did not have full coverage of all GNSS receivers as the map was not complete. It is worth mentioning that during this period the equatorial anomaly is observed.